



HAL
open science

About the transfert matrix method in the context of acoustical wave propagation in wind instruments

Juliette Chabassier, Robin Tournemenne

► To cite this version:

Juliette Chabassier, Robin Tournemenne. About the transfert matrix method in the context of acoustical wave propagation in wind instruments. [Research Report] RR-9254, INRIA Bordeaux. 2019. ⟨hal-02019515⟩

HAL Id: hal-02019515

<https://inria.hal.science/hal-02019515v1>

Submitted on 14 Feb 2019

HAL is a multi-disciplinary open access archive for the deposit and dissemination of scientific research documents, whether they are published or not. The documents may come from teaching and research institutions in France or abroad, or from public or private research centers.

L'archive ouverte pluridisciplinaire **HAL**, est destinée au dépôt et à la diffusion de documents scientifiques de niveau recherche, publiés ou non, émanant des établissements d'enseignement et de recherche français ou étrangers, des laboratoires publics ou privés.



HAL Authorization



About the transfert matrix method in the context of acoustical wave propagation in wind instruments

Juliette Chabassier, Robin Tournemene

**RESEARCH
REPORT**

N° 9254

September 2018

Project-Team Magique-3D



About the transfert matrix method in the context of acoustical wave propagation in wind instruments

Juliette Chabassier, Robin Tournemenne

Project-Team Magique-3D

Research Report n° 9254 — September 2018 — 16 pages

Abstract: The transfer matrix method allows to compute the input impedance of a pipe. This work proposes a unified formulation of the coefficients of the transfer matrices for cones and cylinders. This is done for both models with and without viscothermal losses. The exactly solved equation with the transfer matrix method in the case of the cone with viscothermal losses is exhibited.

Key-words: Acoustics, input impedance, transfer matrix, losses

**RESEARCH CENTRE
BORDEAUX – SUD-OUEST**

200 avenue de la Vieille Tour
33405 Talence Cedex

À propos de la méthode des matrices de transfert dans le contexte de la propagation des ondes acoustiques dans les instruments à vent

Résumé : La méthode des matrices de transfert permet de calculer l'impédance d'entrée d'un tuyau. Ce travail propose une formulation unifiée des coefficients des matrices de transfert pour les cas du cône et du cylindre. Ceci est fait pour les deux modèles avec et sans pertes viscothermiques. L'équation exactement résolue par la méthode des matrices de transfert dans le cas du cône en présence de pertes viscothermiques est exhibée.

Mots-clés : Acoustique, impédance d'entrée, matrice de transfert, pertes

Contents

1	Lossless transfer matrix method	3
1.1	Problem definition	3
1.2	Transfert matrix principle	5
1.3	Transfer matrices for the cylinder and the cone	5
1.4	Seamless formulation of cone and cylinder transfer matrix	7
2	Transfer matrix method considering visco-thermal losses	7
2.1	Problem definition and transfer matrix of the cylinder	7
2.2	Actual problem definition of the cone transfer matrix	8
2.3	Seamless formulation of cone and cylinder transfer matrix	10
A	Webster’s horn equation obtention	11
B	Equivalent formulation of the cone transfer matrix	13
C	Approximated propagation equations for the cone transfer matrix considering visco-thermal losses	13

1 Lossless transfer matrix method

1.1 Problem definition

Consider an axisymmetric pipe occupying a domain $\Omega \subset \mathbb{R}^3 = (Ox, Oy, Oz)$ of slowly varying cross section S and rigid walls developing along the x axis, filled with a fluid, see Figure 1.

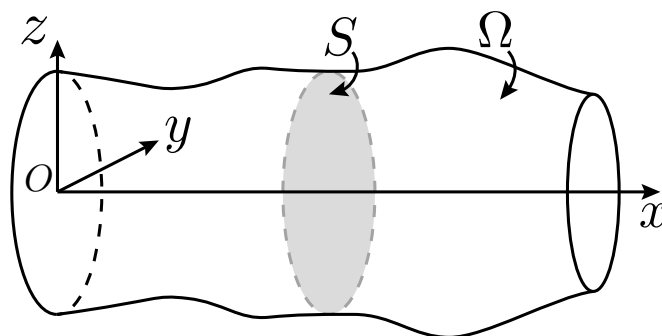


Figure 1: Definition of the space variables. S is the slowly varying section of the axisymmetric pipe

The acoustic pressure $p(x, y, z, t)$ and the three-dimensional flow $u(x, y, z, t)$ can be considered as the solution to Euler three-dimensional equations which are computationally intensive to solve, especially when only the propagating phenomena are of interest. An asymptotic analysis from Euler’s equations for a perfect gas in a pipe with a slowly varying section [10] leads to the classical one-dimensional Webster’s horn equation. We recall the development of this analysis in the Appendix A. The pressure can then be considered as constant in the sections orthogonal to the x -axis, the orthogonal components of the three-dimensional flow can be neglected in

Sound velocity: $c = 331.45\sqrt{T/T_0}$ m s ⁻¹
Density: $\rho = 1.2929 T_0/T$ kg m ⁻³
Viscosity: $\mu = 1.708 e - 5(1 + 0.0029 t)$ kg m ⁻¹ s ⁻¹
Th. cdt.: $\kappa = 5.77 e - 3(1 + 0.0033 t)$ Cal/(ms °C)
Spec. heat with cst. p.: $C_p = 240$ Cal/(kg °C)
Ratio of specific heats: $\gamma = 1.402$

Table 1: Numerical values of air constants used in the model, see [3]. t is the temperature in Celsius, and T the absolute temperature knowing that $T_0 = 273.15^\circ$ K.

the equations while the axial component can be considered as axisymmetric with an analytic expression of its radial dependency. Thus we seek in the frequency domain $\hat{p}(x, \omega)$ the **acoustic pressure** and $\hat{u}(x, \omega)$ the **volume flow** such that the one-dimensional volumic equations read, for all $x \in [0, L]$ and with $k = \omega/c$

$$\begin{cases} \frac{1}{S} \frac{d}{dx} \left(S \frac{d\hat{p}}{dx} \right) + k^2 \hat{p} = 0, & (1a) \\ \frac{j\omega\rho}{S} \hat{u} + \frac{d\hat{p}}{dx} = 0, & (1b) \end{cases}$$

where j is the complex number, ρ the density and c the sound velocity (Table 1 defines the air constants). Where the section S is not discontinuous, it can also be written

$$\begin{cases} k^2 \hat{p} + \frac{1}{S} \frac{dS}{dx} \frac{d\hat{p}}{dx} + \frac{d^2 \hat{p}}{dx^2} = 0, & (2a) \\ \frac{j\omega\rho}{S} \hat{u} + \frac{d\hat{p}}{dx} = 0, & (2b) \end{cases}$$

Two boundary conditions complete the problem: at the bell $x = L$, we impose a radiation impedance [4, 8, 3]:

$$\frac{\hat{p}(L, \omega)}{\hat{u}(L, \omega)} = Z_R(\omega), \quad (3)$$

and at the input of the pipe, we impose

$$\hat{u}(0, \omega) = \lambda(\omega), \quad (4)$$

where $\lambda(\omega)$ will be a source term for the system. Since all the considered equations are linear, we can consider without loss of generality $\lambda(\omega) \equiv 1$. In this work, we are interested in computing the input impedance

$$Z(\omega) := \frac{\hat{p}(0, \omega)}{\hat{u}(0, \omega)}, \quad (5)$$

which is primarily linked to the bore $S : x \rightarrow S(x)$, which is a coefficient in Equations (2). Finally, the considered problem is the following:

$$\text{Compute } Z(\omega) = \frac{\hat{p}(0, \omega)}{\hat{u}(0, \omega)}, \quad \text{where} \quad (6)$$

$$\left\{ \begin{array}{l} \frac{1}{S} \frac{d}{dx} \left(S \frac{d\hat{p}}{dx} \right) + k^2 \hat{p} = 0, \\ \frac{j\omega\rho}{S} \hat{u} + \frac{d\hat{p}}{dx} = 0, \end{array} \right. \quad \forall x \in [0, L] \quad (7a)$$

$$\hat{u}(0, \omega) = 1, \quad (7b)$$

$$\frac{\hat{p}(L, \omega)}{\hat{u}(L, \omega)} = Z_R(\omega). \quad (7c)$$

1.2 Transfert matrix principle

The transfer matrix method (TMM) consists in writing relations between output and input acoustic variables of simple geometries (eg. cylindrical, conical parts, Bessel or exponential bores ...) from the use of the propagation equations [2]. Consequently, given a radiation impedance $Z_R(\omega)$ and discretizing the bore profile in a series of N_p parts, it is possible to compute the instrument's input impedance. Let $\{x_i\}_{0 \leq i \leq N_p}$ be the list of positions on the bore's axis defining all the parts (with $x_0 = 0$ and $x_{N_p} = L$). We also define $\hat{p}_i(\omega)$ and $\hat{u}_i(\omega)$ as approximations of the pressure and the volume flow calculated by the TMM at the positions x_i . When the TMM is exact, $\hat{p}_i(\omega) = \hat{p}(x_i, \omega)$ and $\hat{u}_i(\omega) = \hat{u}(x_i, \omega)$.

Formally, the relation between the input and the output of one simple geometry can be expressed as a 2×2 matrix $T_{i+1}(\omega)$:

$$\begin{pmatrix} \hat{p}_i(\omega) \\ \hat{u}_i(\omega) \end{pmatrix} = \begin{pmatrix} a_{i+1}(\omega) & b_{i+1}(\omega) \\ c_{i+1}(\omega) & d_{i+1}(\omega) \end{pmatrix} \begin{pmatrix} \hat{p}_{i+1}(\omega) \\ \hat{u}_{i+1}(\omega) \end{pmatrix} = T_{i+1}(\omega) \begin{pmatrix} \hat{p}_{i+1}(\omega) \\ \hat{u}_{i+1}(\omega) \end{pmatrix}. \quad (8)$$

We then deduce the relation between the input and the output of the pipe:

$$\zeta = \begin{pmatrix} \hat{p}_0(\omega)/\hat{u}_L(\omega) \\ \hat{u}_0(\omega)/\hat{u}_L(\omega) \end{pmatrix} = \prod_{i=1}^{N_p} T_i(\omega) \begin{pmatrix} Z_R(\omega) \\ 1 \end{pmatrix}. \quad (9)$$

where $\hat{u}_L(\omega)$ is the volume flow at the pipe end, and finally $Z_{\text{TMM}} = \frac{\zeta(1)}{\zeta(2)}$. The global transfer matrix is defined as the product of all the elementary matrices T_i . An implicit transmission condition is therefore assumed, which is the continuity of the variables between all parts. In practice, the computation is done only for a discrete set of pulsations $\{\omega_j\}_{1 \leq j \leq N_\omega}$.

1.3 Transfer matrices for the cylinder and the cone

Cylinder. In the case of an infinite cylinder of section S , the Webster's horn equation of propagation simplifies to the classical one dimensional wave equation

$$\frac{d^2 \hat{p}}{dx^2} + k^2 \hat{p} = 0, \quad (10)$$

where $k = \omega/c$.

An analysis of the solution of this equation shows that the transfer matrix between two positions separated by the distance ℓ is:

$$a_i(\omega) = a, \quad b_i(\omega) = b, \quad c_i(\omega) = c, \quad d_i(\omega) = d, \quad \text{where}$$

$$\begin{cases} a = \cos(k\ell), \\ b = jZ_c \sin(k\ell), \\ c = \frac{j}{Z_c} \sin(k\ell), \\ d = \cos(k\ell), \end{cases}$$

where $Z_c = \rho c/S$. The analysis leading to this formula is notably written in the chapter 2 of [1].

Cone. In the case of a cone, it is somehow more delicate to obtain the transfer matrix, see Appendix A of [1]. Let us consider a cone part defined by two sections of radii R_i and R_{i+1} normal to the cone's axis and separated by a distance ℓ . A change of coordinate is useful to derive the analytical solution. The new axis origin is chosen as the cone apex and is defined so that the new coordinate \tilde{x}_i and \tilde{x}_{i+1} respectively associated with the radii R_i and R_{i+1} satisfy $\tilde{x}_i < \tilde{x}_{i+1}$ (with $\ell = \tilde{x}_{i+1} - \tilde{x}_i$), see Figure 2. One gets that the corresponding transfer matrix of a divergent or convergent cone part reads:

$$a_i(\omega) = a, \quad b_i(\omega) = b, \quad c_i(\omega) = c, \quad d_i(\omega) = d, \quad \text{where}$$

$$\begin{cases} a = \frac{\tilde{x}_{i+1}}{\tilde{x}_i} \cos k\ell - \frac{1}{k} \frac{\sin k\ell}{\tilde{x}_i}, & (12a) \\ b = \frac{\tilde{x}_i}{\tilde{x}_{i+1}} j Z_{c,i} \sin k\ell, & (12b) \\ c = \frac{j}{Z_{c,i}} \left[\left(\frac{\tilde{x}_{i+1}}{\tilde{x}_i} + \frac{1}{k^2} \frac{\sin k\ell}{\tilde{x}_i^2} \right) \sin k\ell - \frac{\ell}{k} \frac{\cos k\ell}{\tilde{x}_i^2} \right], & (12c) \\ d = \frac{\tilde{x}_i}{\tilde{x}_{i+1}} \left(\cos k\ell + \frac{1}{k} \frac{\sin k\ell}{\tilde{x}_i} \right), & (12d) \end{cases}$$

with $Z_{c,i} = \rho c / (\pi R_i^2)$.

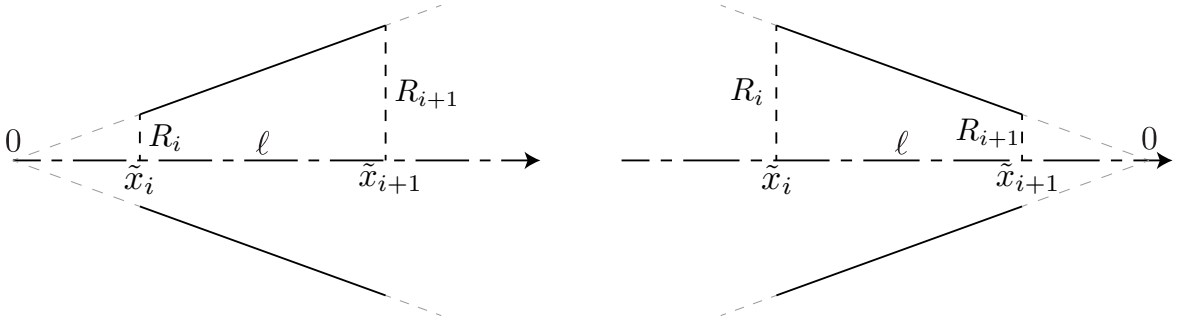


Figure 2: Definition of the geometrical quantities for a divergent cone and a convergent cones. Notice that \tilde{x}_i and \tilde{x}_{i+1} are negative for the convergent cone.

This formula is exactly the transfer matrix formula that can be found in [7]. An equivalent formula is sometimes used in the community (section 7.4.3 from [3]) and the transition from one formulation to the other can be found in the Appendix B.

1.4 Seamless formulation of cone and cylinder transfer matrix

The cone formulation (12) does not converge towards the cylinder formulation when $R_i \rightarrow R_{i+1}$ because \tilde{x}_i and \tilde{x}_{i+1} go towards infinity. Taking into account the geometrical relations, it is possible to overcome this problem providing one single transfer matrix formula for both cone and cylinder cases:

The transfer matrix of a cone or cylinder part of length ℓ with input radius R_i and output radius R_{i+1} is given by:

$$T_{i+1}(\omega) = \begin{pmatrix} a_{i+1}(\omega) & b_{i+1}(\omega) \\ c_{i+1}(\omega) & d_{i+1}(\omega) \end{pmatrix}$$

where

$$\left\{ \begin{array}{l} a_{i+1}(\omega) = \frac{R_{i+1}}{R_i} \cos k\ell - \frac{\beta}{k} \sin k\ell, \end{array} \right. \quad (13a)$$

$$\left\{ \begin{array}{l} b_{i+1}(\omega) = \frac{R_i}{R_{i+1}} j Z_{c,i} \sin k\ell, \end{array} \right. \quad (13b)$$

$$\left\{ \begin{array}{l} c_{i+1}(\omega) = \frac{j}{Z_{c,i}} \left[\left(\frac{R_{i+1}}{R_i} + \frac{\beta^2}{k^2} \right) \sin k\ell - \frac{\ell\beta^2}{k} \cos k\ell \right], \end{array} \right. \quad (13c)$$

$$\left\{ \begin{array}{l} d_{i+1}(\omega) = \frac{R_i}{R_{i+1}} \left(\cos k\ell + \frac{\beta}{k} \sin k\ell \right). \end{array} \right. \quad (13d)$$

$$\left\{ \begin{array}{l} \beta = \frac{R_{i+1} - R_i}{\ell R_i}, \quad k = \frac{\omega}{c}, \quad Z_{c,i} = \frac{\rho c}{\pi R_i^2} \end{array} \right. \quad (13e)$$

$$\left\{ \begin{array}{l} \beta = \frac{R_{i+1} - R_i}{\ell R_i}, \quad k = \frac{\omega}{c}, \quad Z_{c,i} = \frac{\rho c}{\pi R_i^2} \end{array} \right. \quad (13f)$$

$$\left\{ \begin{array}{l} \beta = \frac{R_{i+1} - R_i}{\ell R_i}, \quad k = \frac{\omega}{c}, \quad Z_{c,i} = \frac{\rho c}{\pi R_i^2} \end{array} \right. \quad (13g)$$

$$\beta = \frac{R_{i+1} - R_i}{\ell R_i}, \quad k = \frac{\omega}{c}, \quad Z_{c,i} = \frac{\rho c}{\pi R_i^2} \quad (14)$$

Notice that this formula does not diverge when R_i is equal to R_{i+1} and that β can be interpreted in the previous definitions as $\beta = \frac{1}{\tilde{x}_i}$.

2 Transfer matrix method considering visco-thermal losses

2.1 Problem definition and transfer matrix of the cylinder

It is possible to take into account in a one dimensional model the visco-thermal losses induced by the pipe's wall thanks to a simplification of Kirchhoff's theory [5, 11, 3]. This model has been derived for cylinders but is also used for slowly varying cross section S . The propagation equations become, for all position $x \in [0, L]$ and pulsation ω ,

$$\begin{cases} Z_v(\omega, x) \hat{u} + \frac{d\hat{p}}{dx} = 0, \\ Y_t(\omega, x) \hat{p} + \frac{d\hat{u}}{dx} = 0, \end{cases} \quad (15a)$$

$$(15b)$$

with

$$\begin{cases} Z_v(\omega, x) = \frac{j\omega\rho}{S(x)} [1 - \mathcal{J}(k_v(\omega)R(x))]^{-1}, \\ Y_t(\omega, x) = \frac{j\omega S(x)}{\rho c^2} [1 + (\gamma - 1)\mathcal{J}(k_t(\omega)R(x))], \end{cases} \quad (16a)$$

$$(16b)$$

$$k_v(\omega) = \sqrt{j\omega\frac{\rho}{\mu}}, \quad k_t(\omega) = \sqrt{j\omega\rho\frac{C_p}{\kappa}},$$

where $R(x)$ is the section radius, $S(x) = \pi R(x)^2$ is the section area, table 1 describes the air constants, and we introduce the function \mathcal{J} of a complex variable, which models the dissipative terms, as

$$\mathcal{J}(z) = \frac{2 J_1(z)}{z J_0(z)}, \quad \forall z \in \mathbb{C}. \quad (17)$$

J_1 and J_0 are respectively the first kind Bessel functions of first and zero order. The same boundary conditions as in the previous section completes this problem.

One can notice that if the dissipative terms are neglected, this model formally tends to the previous Webster's horn equations, which shows the compatibility of the two models. Unfortunately, the function \mathcal{J} being non-linear, there is, to the best of our knowledge, no way to derive exact analytical formulas for any other pipe's geometries than for the cylinder, for which Z_v and Y_t are constant with respect to x .

The exact transfer matrix of a cylinder of section S between two positions distant of ℓ is:

$$\begin{cases} a = \cosh(\Gamma\ell), \\ b = jZ_c \sin(k\ell), \\ c = \frac{j}{Z_c} \sin(k\ell), \\ d = \cos(k\ell), \end{cases}$$

where $\Gamma = \sqrt{Z_v Y_t}$ and $Z_c = \sqrt{Z_v / Y_t}$ (which is equal to $\rho c / S$ if the losses are neglected). One can observe that this transfer matrix is formally identical to the transfer matrix in the lossless case replacing jk by Γ and Z_c by its corresponding definition.

2.2 Actual problem definition of the cone transfer matrix

Two empirical strategies exist to derive approximated transfer matrices for the cone considering visco-thermal losses at the pipe's wall. A first empirical approach handles this difficulty for conical parts by approximating them as a succession of cylinders of increasing or decreasing radii [2]. A second empirical approach proposes to discretize each conical part in N_{sub} smaller cones, and to use on each subdivision the transfer matrix derived for the cone considering lossless propagation, replacing some parameters by their lossy counterparts evaluated at a chosen intermediate radius

R^\odot [7, 1]. For a bore initially made of N_p conical parts, the total number of actual transfer matrices to compute would be $N_{\text{TMM}} = N_p \times N_{\text{sub}}$.

Since the visco-thermal losses depend non-linearly on the radius, no optimal value for R^\odot can be immediately derived. Possible choices are the average radius $R^\odot = (R_i + R_{i+1})/2$ as in [7] (where R_i and R_{i+1} are the input and output radii of the small cone), or any other weighted average. In this report, we choose $R^\odot = (2 \min(R_i, R_{i+1}) + \max(R_i, R_{i+1}))/3$, which seems to be used in some existing implementations of the TMM.

As shown in Appendix C, using the TMM with the approximate matrix obtained with this strategy corresponds to actually solving analytically the following system of equations: compute

$$Z_{\text{TMM}}(\omega) = \frac{\check{p}(0, \omega)}{\check{u}(0, \omega)}, \text{ where } \forall i \in [1, N_{\text{TMM}}], \quad (19)$$

$$\left\{ \begin{array}{l} Z_v^i \check{u} + \frac{d\check{p}}{dx} = 0, \\ Y_t^i \check{p} + \frac{d\check{u}}{dx} = 0, \end{array} \quad \forall x \in [x_i, x_{i+1}] \right. \quad (20a)$$

$$Z_v^i = \frac{j\omega \rho}{S} [1 - \mathcal{J}(k_v(\omega) R_i^\odot)]^{-1}, \quad (20b)$$

$$Y_t^i = \frac{j\omega S}{\rho c^2} [1 + (\gamma - 1) \mathcal{J}(k_t(\omega) R_i^\odot)], \quad (20c)$$

$$\check{p}(x_i^+) = \check{p}(x_i^-), \quad \check{u}(x_i^+) = \check{u}(x_i^-), \quad (20d)$$

$$R_i^\odot = (2 \min(R(x_i), R(x_{i+1})) + \max(R(x_i), R(x_{i+1}))) / 3, \quad (20e)$$

$$\check{u}(0, \omega) = 1, \quad (20f)$$

$$\left. \begin{array}{l} \frac{\check{p}(L, \omega)}{\check{v}(L, \omega)} = Z_R(\omega). \end{array} \right\} \quad (20g)$$

This problem is different from the continuous problem (15) solved with the FEM. The difference lies in the approximation R^\odot inside the function \mathcal{J} for every interval $[x_i, x_{i+1}]$ and amounts to approximating the original equation coefficients with discontinuous ones.

2.3 Seamless formulation of cone and cylinder transfer matrix

Finally, we propose a unified formulation for the computation of the transfer matrix $T_i(\omega)$, equivalent to the ones of the literature [7], for cones and cylinders under visco-thermal losses. It reads:

The transfer matrix of a cone or cylinder part of length ℓ with input radius R_i and output radius R_{i+1} is given by:

$$T_{i+1}(\omega) = \begin{pmatrix} a_{i+1}(\omega) & b_{i+1}(\omega) \\ c_{i+1}(\omega) & d_{i+1}(\omega) \end{pmatrix}$$

where

$$a_{i+1}(\omega) = \frac{R_{i+1}}{R_i} \cosh \Gamma_i \ell - \frac{\beta}{\Gamma_i} \sinh \Gamma_i \ell \quad (21a)$$

$$b_{i+1}(\omega) = \frac{R_i}{R_{i+1}} Z_{c,i} \sinh \Gamma_i \ell \quad (21b)$$

$$c_{i+1}(\omega) = \frac{1}{Z_{c,i}} \left[\left(\frac{R_{i+1}}{R_i} - \frac{\beta^2}{\Gamma_i^2} \right) \sinh \Gamma_i \ell + \frac{\beta^2 \ell}{\Gamma_i} \cosh \Gamma_i \ell \right] \quad (21c)$$

$$d_{i+1}(\omega) = \frac{R_i}{R_{i+1}} \left(\cosh \Gamma_i \ell + \frac{\beta}{\Gamma_i} \sinh \Gamma_i \ell \right) \quad (21d)$$

where

$$\Gamma_i \equiv \Gamma(\omega, R_i^\odot) = \frac{j\omega}{c} \sqrt{\frac{1 + (\gamma - 1)\mathcal{J}(k_t(\omega)R_i^\odot)}{1 - \mathcal{J}(k_v(\omega)R_i^\odot)}},$$

$$Z_{c,i} \equiv Z_c(\omega, R_i^\odot) = \frac{\rho c}{\pi R_i^2} \sqrt{\frac{[1 + (\gamma - 1)\mathcal{J}(k_t(\omega)R_i^\odot)]^{-1}}{1 - \mathcal{J}(k_v(\omega)R_i^\odot)}}$$

and

$$\beta = \frac{R_{i+1} - R_i}{\ell R_i}. \quad (22)$$

References

- [1] Alistair Charles Peter Braden. *Bore optimisation and impedance modelling of brass musical instruments*. PhD thesis, University of Edinburgh, 2007.
- [2] René Caussé, J Kergomard, and X Lurton. Input impedance of brass musical instruments—comparison between experiment and numerical models. *J. Acoust. Soc. Am.*, 75(1):241–254, 1984.
- [3] Antoine Chaigne and Jean Kergomard. *Acoustics of Musical Instruments*. Modern Acoustics and Signal Processing. Springer New York, 2016.
- [4] Jean-Pierre Dalmont, Cornelis J Nederveen, and Nicolas Joly. Radiation impedance of tubes with different flanges: Numerical and experimental investigations. *Journal of Sound and Vibration*, 244(3):505 – 534, 2001.

- [5] Gustav Kirchhoff. Ueber den einfluss der wärmeleitung in einem gase auf die schallbewegung. *Annalen der Physik*, 210(6):177–193, 1868.
- [6] M.B. Lesser and D.G. Crighton. Physical acoustics and the method of matched asymptotic expansions. *Physical Acoustics*, 11:69 – 149, 1975. Physical Acoustics.
- [7] Dan Mapes-Riordan. Horn modeling with conical and cylindrical transmission-line elements. *J. Audio Eng. Soc.*, 41(6):471–484, 1993.
- [8] Lawrence R Rabiner and Ronald W Schafer. *Digital processing of speech signals*, volume 100. Prentice-hall Englewood Cliffs, NJ, 1978.
- [9] S W Sjoerd Rienstra and A Avraham Hirschberg. *An introduction to acoustics*. Technische Universiteit Eindhoven, 2004.
- [10] Sjoerd W Rienstra. Webster’s horn equation revisited. *SIAM Journal on Applied Mathematics*, 65(6):1981–2004, 2005.
- [11] Cornelis Zwikker and Cornelis Willem Kosten. *Sound absorbing materials*. Elsevier, 1949.

A Webster’s horn equation obtention

The following appendix is a synthesis of a part of the article [10]. In the acoustic realm of a perfect gas, the pressure \tilde{p} , the fluid velocity $\tilde{\mathbf{v}}$, the density $\tilde{\rho}$, the entropy \tilde{s} , the sound speed \tilde{c} verify the mass conservation (with no source),

$$\operatorname{div} \tilde{\rho} \tilde{\mathbf{v}} + \frac{\partial \tilde{\rho}}{\partial t} = 0, \quad (23)$$

the momentum conservation (with no external force),

$$\tilde{\rho} \frac{\partial \tilde{\mathbf{v}}}{\partial t} = -\operatorname{grad} \tilde{p}, \quad (24)$$

the isentropic flow,

$$\frac{d\tilde{s}}{dt} = 0, \quad (25)$$

and the state equations of a perfect gas,

$$d\tilde{s} = C_v \frac{d\tilde{p}}{\tilde{p}} - C_p \frac{d\tilde{\rho}}{\tilde{\rho}}, \quad \tilde{c}^2 = \frac{\gamma \tilde{p}}{\tilde{\rho}}, \quad \gamma = \frac{C_p}{C_v}, \quad (26)$$

where γ , C_p and C_v are gas constants. Assuming an unsteady time-harmonic perturbation of frequency ω we can study these equations setting $\tilde{p} = P + \hat{p}e^{j\omega t}$, $\tilde{\mathbf{v}} = \mathbf{v}_0 + \mathbf{v}e^{j\omega t}$, $\tilde{\rho} = \rho + \rho'e^{j\omega t}$, $\tilde{s} = s_0 + se^{j\omega t}$, $\tilde{c} = c + c'e^{j\omega t}$. If we neglect the mean flow ($\mathbf{v}_0 = 0$) and suppose the density and the sound speed constant ($\rho' = c' = 0$, c, ρ constant) we obtain, after manipulations [9], the classical acoustic wave equation:

$$\nabla^2 \hat{p} + k^2 \hat{p} = 0, \quad (27)$$

where $k = \omega/c$ is the wave number. This rather general equation is studied for a duct of arbitrary cross section S slowly varying along the axis x , see Figure 1. In order to find an approximated one-dimensional model in this context, an asymptotically systematic derivation of

the three-dimensional classic problem is utilized ([6, 10, 9]). The duct dimension along the x axis being large compared to the cross section dimensions, a so-called slow variable $X = \epsilon x \geq 0$ is used - the small number ϵ is the Helmholtz number, the ratio between the duct diameter and the typical wavelength. Consequently, a variation of X is comparable to a cross section variation. This mathematical shrink of the duct, induces a wavelength contraction, which leads us to use the new wave number $\kappa = k/\epsilon$. In cylindrical coordinates, the duct radius is described by the function $R(X, \theta)$. Consequently, the function

$$V_{\text{ol}} = r - R(X, \theta), \quad (28)$$

represents the points inside the duct if $V_{\text{ol}} < 0$ and any point on the surface if $V_{\text{ol}} = 0$. On the duct surface ($V_{\text{ol}} = 0$), the gradient ∇V_{ol} is a vector normal to the surface ([9], section A.3). At the solid wall, we have the boundary condition of vanishing normal velocity:

$$\nabla \hat{p} \cdot \nabla V_{\text{ol}} = 0, \quad \text{at } V_{\text{ol}} = 0. \quad (29)$$

Under the new variables, the acoustic wave equation becomes

$$\nabla^2 \hat{p} + \epsilon^2 \kappa^2 \hat{p} = 0. \quad (30)$$

Assuming the asymptotic expansion

$$\hat{p}(X, r, \theta, \epsilon) = \hat{p}_0(X, r, \theta) + \epsilon^2 \hat{p}_1(X, r, \theta) + \mathcal{O}(\epsilon^4). \quad (31)$$

Using Eq. (29) and (30), it is then possible to demonstrate that the leading order p_0 is solution to Webster's horn equation:

$$\frac{1}{S} \frac{d}{dx} \left(S \frac{d\hat{p}_0}{dx} \right) + k^2 \hat{p}_0 = 0, \quad (32)$$

where S is the cross section area at position x .

The initial model bears two approximations: the gas is perfect and the momentum conservation is dealt thanks to the Material derivative. Under this model, thanks to the asymptotic expansion we know that the error made approximating \hat{p} by \hat{p}_0 is in $\mathcal{O}(\epsilon^2)$. Finally, in this report we consider only the leading order ($\hat{p} \sim \hat{p}_0$), consequently, the Webster's horn equation reads

$$\frac{1}{S} \frac{d}{dx} \left(S \frac{d\hat{p}}{dx} \right) + k^2 \hat{p} = 0, \quad (33)$$

at the second order in space, and it is possible to introduce \hat{u} such that

$$\begin{cases} \frac{j\omega\rho}{S} \hat{u} + \frac{d\hat{p}}{dx} = 0, & (34a) \\ \frac{j\omega S}{\rho c^2} \hat{p} + \frac{d\hat{u}}{dx} = 0, & (34b) \end{cases}$$

at the first order in space, where \hat{u} is called the volume flow.

B Equivalent formulation of the cone transfer matrix

The transfer matrix found in [7] reads

$$\left\{ \begin{array}{l} a = \frac{\tilde{x}_{i+1}}{\tilde{x}_i} \cos k\ell - \frac{\sin k\ell}{k\tilde{x}_i}, \end{array} \right. \quad (35a)$$

$$\left\{ \begin{array}{l} b = \frac{\tilde{x}_i}{\tilde{x}_{i+1}} j Z_{c,i} \sin k\ell, \end{array} \right. \quad (35b)$$

$$\left\{ \begin{array}{l} c = \frac{j}{Z_{c,i}} \left[\left(\frac{\tilde{x}_{i+1}}{\tilde{x}_i} + \frac{1}{k^2 \tilde{x}_i^2} \right) \sin k\ell - \frac{\ell}{k\tilde{x}_i^2} \cos k\ell \right], \end{array} \right. \quad (35c)$$

$$\left\{ \begin{array}{l} d = \frac{\tilde{x}_i}{\tilde{x}_{i+1}} \left(\cos k\ell + \frac{1}{k\tilde{x}_i} \sin k\ell \right), \end{array} \right. \quad (35d)$$

$Z_{c,i}$ being the characteristic impedance at the entrance: $Z_c = \rho c / (\pi R_i^2)$.
This is equivalent to (using Thales theorem)

$$\left\{ \begin{array}{l} a = \frac{R_{i+1}}{R_i} \cos k\ell - \frac{\sin k\ell}{k\tilde{x}_i}, \end{array} \right. \quad (36a)$$

$$\left\{ \begin{array}{l} b = \frac{R_i}{R_{i+1}} j \frac{\rho c}{\pi R_i^2} \sin k\ell, \end{array} \right. \quad (36b)$$

$$\left\{ \begin{array}{l} c = \frac{j}{\rho c} \left[\left(R_i R_{i+1} + \frac{1}{k^2} \right) \sin k\ell - \frac{\ell}{k} \cos k\ell \right], \end{array} \right. \quad (36c)$$

$$\left\{ \begin{array}{l} d = \frac{R_i}{R_{i+1}} \cos k\ell + \frac{1}{k\tilde{x}_{i+1}} \sin k\ell, \end{array} \right. \quad (36d)$$

which is equivalent to the formulation found in section 7.4.3 of [3]¹:

$$\left\{ \begin{array}{l} a = \frac{R_{i+1}}{R_i} \cos k\ell - \frac{\sin k\ell}{k\tilde{x}_i}, \end{array} \right. \quad (37a)$$

$$\left\{ \begin{array}{l} b = j \frac{\rho c}{\pi R_i R_{i+1}} \sin k\ell, \end{array} \right. \quad (37b)$$

$$\left\{ \begin{array}{l} c = \frac{\pi R_i R_{i+1}}{\rho c} \left[\left(1 + \frac{1}{k^2 \tilde{x}_i \tilde{x}_{i+1}} \right) j \sin k\ell - \frac{\cos k\ell}{jk} \left(\frac{1}{\tilde{x}_i} - \frac{1}{\tilde{x}_{i+1}} \right) \right], \end{array} \right. \quad (37c)$$

$$\left\{ \begin{array}{l} d = \frac{R_i}{R_{i+1}} \cos k\ell + \frac{\sin k\ell}{k\tilde{x}_{i+1}}. \end{array} \right. \quad (37d)$$

C Approximated propagation equations for the cone transfer matrix considering visco-thermal losses

In this section, the $\tilde{\cdot}$ on positions x are removed for ease of reading.

¹In their equation the definition of ℓ should be equal to $\tilde{x}_{i+1} - \tilde{x}_i$

The aim is to prove that the system (20) is indeed leading to the transfer matrices proposed by [7]. For the demonstration, we will start from the propagation equations and show that they lead to the given transfer matrix.

The complete system we are analyzing is $\forall i \in [1, N_{\text{TMM}}]$,

$$\left\{ \begin{array}{l} \left\{ \begin{array}{l} Z_v^i \check{u} + \frac{d\check{p}}{dx} = 0, \\ Y_t^i \check{p} + \frac{d\check{u}}{dx} = 0, \end{array} \right. \quad \forall x \in [x_i, x_{i+1}] \\ \\ Z_v^i = \frac{j\omega\rho}{S} [1 - \mathcal{J}(k_v(\omega)R_i^\odot)]^{-1}, \\ \check{p}(x_i) = \check{p}(x_{i+1}), \quad \check{u}(x_i) = \check{u}(x_{i+1}), \\ Y_t^i = \frac{j\omega S}{\rho c^2} [1 + (\gamma - 1)\mathcal{J}(k_t(\omega)R_i^\odot)], \\ R_i^\odot = (2 \min(R(x_i), R(x_{i+1})) + \max(R(x_i), R(x_{i+1}))) / 3, \\ \check{u}(0, \omega) = 1, \\ \frac{\check{p}(L, \omega)}{\check{v}(L, \omega)} = Z_R(\omega). \end{array} \right.$$

We differentiate with respect to x the first equation of system (20):

$$\left\{ \begin{array}{l} Z_v^i \frac{d\check{u}}{dx} + \check{u} j\omega\rho [1 - \mathcal{J}(k_v(\omega)R_i^\odot)]^{-1} \frac{d}{dx} \left(\frac{1}{S} \right) + \frac{d^2\check{p}}{dx^2} = 0, \end{array} \right. \quad (39a)$$

$$\left\{ \begin{array}{l} Y_t^i \check{p} + \frac{d\check{u}}{dx} = 0, \end{array} \right. \quad (39b)$$

using Equation (39b) and the first equation of system (20) in (39a):

$$\left\{ \begin{array}{l} -Z_v^i Y_t^i \check{p} - \frac{d\check{p}}{dx} \frac{S}{j\omega\rho [1 - \mathcal{J}(k_v(\omega)R_i^\odot)]^{-1}} j\omega\rho [1 - \mathcal{J}(k_v(\omega)R_i^\odot)]^{-1} \left(-\frac{1}{S^2} \right) \frac{dS}{dx} + \frac{d^2\check{p}}{dx^2} = 0, \end{array} \right. \quad (40a)$$

$$\left\{ \begin{array}{l} Z_v^i \check{u} + \frac{d\check{p}}{dx} = 0, \end{array} \right. \quad (40b)$$

We define $\Gamma_i = \sqrt{Z_v^i Y_t^i}$:

$$\left\{ \begin{array}{l} -\Gamma_i^2 \check{p} + \frac{1}{S} \frac{dS}{dx} \frac{d\check{p}}{dx} + \frac{d^2\check{p}}{dx^2} = 0, \end{array} \right. \quad (41a)$$

$$\left\{ \begin{array}{l} Z_v^i \check{u} + \frac{d\check{p}}{dx} = 0, \end{array} \right. \quad (41b)$$

This system of Equations is similar to the system (2). The differences lies in the coefficient $-\Gamma_i^2$ which is $+k^2$ in (2), and the coefficient Z_v^i which is equal to $j\omega\rho/S$ in (2).

We will follow the technique found in the Appendix A of [1] to derive the transfer matrix function of the system (41). Yet, we will study the following broader family of systems:

$$\begin{cases} \alpha\check{p} + \frac{1}{S} \frac{dS}{dx} \frac{d\check{p}}{dx} + \frac{d^2\check{p}}{dx^2} = 0, & (42a) \\ \check{u} = -\beta(x) \frac{d\check{p}}{dx}. & (42b) \end{cases}$$

If α and $\beta(x)$ are respectively equal to k^2 and $S(x)/j\omega\rho$, this system is the Webster's horn propagation equations (2). If α and $\beta(x)$ are respectively equal to $-\Gamma_i^2$ and $1/Z_v^i$, this system is the approximated propagation equations considering visco-thermal losses (41).

In the case of a convergent or divergent cone of slope a whose origin is defined as in Figure 2, $S = \pi(\theta x)^2$ and $\frac{1}{S} \frac{dS}{dx} = \frac{2}{x}$. Equation (42a) becomes

$$\alpha\check{p} + \frac{2}{x} \frac{d\check{p}}{dx} + \frac{d^2\check{p}}{dx^2} = 0 \quad (43)$$

The solution to this equation is

$$\check{p}(x) = \frac{A}{x} e^{-j\delta x} + \frac{B}{x} e^{j\delta x}, \quad (44)$$

where $\delta^2 = \alpha$. This can be reformulated as

$$\check{p} = \frac{1}{x} [(A+B) \cos \delta x - j(A-B) \sin \delta x], \quad (45)$$

and Equation (42b) leads to

$$\check{u} = \beta \left(\frac{1}{x^2} [(A+B) \cos \delta x - j(A-B) \sin \delta x] + \frac{\delta}{x} [(A+B) \sin \delta x + j(A-B) \cos \delta x] \right). \quad (46)$$

We have then the following impedance formula

$$Z(x) = \frac{\frac{1}{x} [(A+B) \cos \delta x - j(A-B) \sin \delta x]}{\beta \left(\frac{1}{x^2} [(A+B) \cos \delta x - j(A-B) \sin \delta x] + \frac{\delta}{x} [(A+B) \sin \delta x + j(A-B) \cos \delta x] \right)}, \quad (47)$$

which leads to

$$\frac{A+B}{A-B} = \frac{j\beta \left[\frac{1}{x} \sin \delta x - \delta \cos \delta x \right] Z(x) - j \sin \delta x}{\beta \left[\frac{1}{x} \cos \delta x + \delta \sin \delta x \right] Z(x) - \cos \delta x} \quad (48)$$

The quotient $\frac{A+B}{A-B}$ is constant w.r.t x . Consequently, defining $Z(x_i)$ and $Z(x_{i+1})$ respectively as Z_0 and Z_1 , we observe the following equality

$$\frac{A+B}{A-B} = \frac{\gamma_1 Z_0 + \gamma_2}{\gamma_3 Z_0 + \gamma_4} = \frac{\gamma_5 Z_1 + \gamma_6}{\gamma_7 Z_1 + \gamma_8}. \quad (49)$$

This leads to the following transfer matrix

$$Z_0 = \frac{[\gamma_1 \gamma_7 - \gamma_3 \gamma_5] Z_1 + \gamma_1 \gamma_8 - \gamma_3 \gamma_6}{[\gamma_4 \gamma_5 - \gamma_2 \gamma_7] Z_1 + \gamma_4 \gamma_6 - \gamma_2 \gamma_8} = \frac{aZ_1 + b}{cZ_1 + d} \quad (50)$$

Using (48), it finally gives

$$\left\{ \begin{array}{l} a = j\beta(x_{i+1}) \left[-\frac{1}{x_{i+1}} \sin \delta \ell + \delta \cos \delta \ell \right] , \\ b = j \sin \delta \ell , \\ c = j\alpha\beta(x_i)\beta(x_{i+1}) \left[-\left(\frac{1}{x_i x_{i+1} \alpha} + 1 \right) \sin \delta \ell + \frac{\ell}{x_i x_{i+1} \delta} \cos \delta \ell \right] , \\ d = j\beta(x_i) \left[\frac{1}{x_i} \sin \delta \ell + \delta \cos \delta \ell \right] , \end{array} \right. \quad \begin{array}{l} (51a) \\ (51b) \\ (51c) \\ (51d) \end{array}$$

where $\ell = x_{i+1} - x_i$.

In the Webster's horn Equation case, replacing α by k^2 and $\beta(x)$ by $S(x)/j\omega\rho$ we find

$$\left\{ \begin{array}{l} a = \frac{\pi\theta^2 x_i x_{i+1}}{\rho c} \frac{x_{i+1}}{x_i} \cos k\ell - \frac{1}{kx_i} \sin k\ell , \\ b = \frac{\pi\theta^2 x_i x_{i+1}}{\rho c} \frac{x_i}{x_{i+1}} jZ_c \sin k\ell , \\ c = \frac{\pi\theta^2 x_i x_{i+1}}{\rho c} \frac{j}{Z_c} \left[\left(\frac{x_{i+1}}{x_i} + \frac{1}{k^2 x_i^2} \right) \sin k\ell - \frac{\ell}{kx_i^2} \cos k\ell \right] , \\ d = \frac{\pi\theta^2 x_i x_{i+1}}{\rho c} \frac{x_i}{x_{i+1}} \left[\cos k\ell + \frac{1}{kx_i} \sin k\ell \right] , \end{array} \right.$$

which, after simplification by $\frac{\pi\theta^2 x_i x_{i+1}}{c\rho}$ gives the formula (12), found in [7].

Similarly, for the approximated visco-thermal case, replacing α by $-\Gamma_i^2$ and $\beta(x)$ by $1/Z_v^i(x)$ we find

$$\left\{ \begin{array}{l} a = \frac{-1}{Z_c(x_{i+1})} \frac{x_i}{x_{i+1}} \frac{x_{i+1}}{x_i} \left[\cosh \Gamma \ell - \frac{1}{\Gamma x_{i+1}} \sinh \Gamma \ell \right] , \\ b = \frac{-1}{Z_c(x_i)} \frac{x_{i+1}}{x_i} \frac{x_i}{x_{i+1}} Z_c(x_i) \sinh \Gamma \ell , \\ c = \frac{-1}{Z_c(x_i)} \frac{x_{i+1}}{x_i} \frac{1}{Z_c(x_i)} \left[\left(\frac{x_{i+1}}{x_i} - \frac{1}{\Gamma^2 x_i^2} \right) \sinh \Gamma \ell + \frac{\ell}{\Gamma x_i^2} \cosh \Gamma \ell \right] , \\ d = \frac{-1}{Z_c(x_i)} \frac{x_{i+1}}{x_i} \frac{x_i}{x_{i+1}} \left[\cosh \Gamma \ell + \frac{1}{\Gamma x_i} \sinh \Gamma \ell \right] , \end{array} \right.$$

observing that $\frac{-1}{Z_c(x_{i+1})} \frac{x_i}{x_{i+1}} = \frac{-1}{Z_c(x_i)} \frac{x_{i+1}}{x_i}$ and simplifying by $\frac{-1}{Z_c(x_i)} \frac{x_{i+1}}{x_i}$, one finds the same expression than [7] and eventually the formula (21). This proves that the propagation equations from (20) are the solved equations. Beside, the other Equations from (20) complete the TMM approach: Equation (20e) setting R^\odot is arbitrary based on empirical observations, Equation (20d) translates the continuity hypothesis made by the transfer matrix method between two parts, and Equations (20f) and (20g) are the necessary boundary condition closing the problem.



**RESEARCH CENTRE
BORDEAUX – SUD-OUEST**

200 avenue de la Vieille Tour
33405 Talence Cedex

Publisher
Inria
Domaine de Voluceau - Rocquencourt
BP 105 - 78153 Le Chesnay Cedex
inria.fr

ISSN 0249-6399

